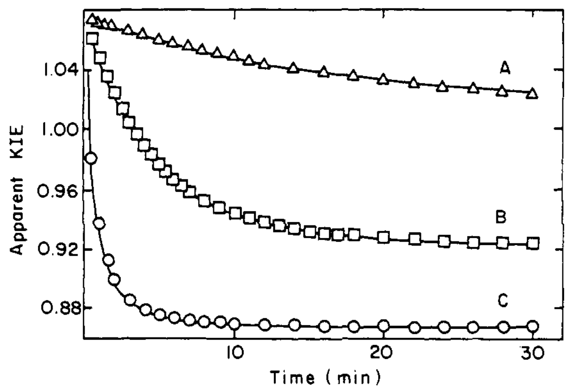

Figure 2. Simulated time dependence of apparent ^{18}O KIE. Simulated curves based on eq 1. $k_1 = 1.0 \times 10^8$, $k_{-1} = 1.0 \times 10^2$, $k_2 = 1.0$ values are identical in all cases, and associated KIE values are set to 1.0. A: $k_3^{16} = 0.005$, $k_{-3}^{16} = 0.05$, $k_4^{16} = 0.1$. B: $k_3^{16} = 0.12$, $k_{-3}^{16} = 0.5$, $k_4^{16} = 0.1$. C: $k_3^{16} = 0.001$, $k_{-3}^{16} = 5.0$, $k_4^{16} = 0.1$. $k_3^{16}/k_3^{18} = 1.075$, $k_{-3}^{16}/k_{-3}^{18} = 1.25$, $k_4^{16}/k_4^{18} = 1.0$ for all simulations.

tope effect in a multistep process. We assume a simple mechanistic model based upon that generally proposed for the serine proteases,[10] with the abbreviations E, enzyme; S, substrate;

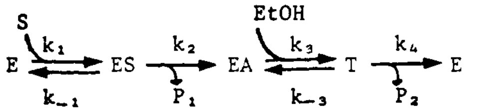
$$E \underset{k_{-1}}{\overset{S\quad k_1}{\rightleftharpoons}} ES \xrightarrow[P_1]{k_2} EA \underset{k_{-3}}{\overset{EtOH\quad k_3}{\rightleftharpoons}} T \xrightarrow[P_2]{k_4} E \qquad (1)$$

ES, enzyme-substrate complex; P_1, *p*-nitrophenol; EA, acylated enzyme; T, a hypothetical species commonly believed to be the tetrahedral intermediate; and P_2, ethyl ester product. With substrate and ethanol in large excess, the rate equations for this scheme become linear, and the explicit integrated form of the equation for the production of P_2 can be obtained.[8] Using this equation, and assigning an arbitrary normal KIE to each of the constants k_3, k_{-3}, and k_4 and reasonable values to all six rate constants, one can generate simulated KIE data which resemble qualitatively the experimental results (Figure 2). The shape of the time-dependent curve depends upon the relative magnitudes of the rate constants, and two conditions are required for a switch from normal to inverse apparent KIE: $^{16}k_{-3}/^{18}k_{-3} > {}^{16}k_3/^{18}k_3$; k_4 not appreciably greater than k_{-3}. These simulated results (which are not intended to reproduce the experimental results quantitatively) support the interpretation that the inverse KIE observed by us is due to a kinetically significant intermediate between the acylated and free enzyme (eq 1). The simulation does not, however, account for the magnitude of the effect. If eq 1 is correct, then the shape of the experimental KIE curve may provide information about the relative magnitudes of the rate constants leading to and away from the hypothetical intermediate T.

Acknowledgments. We are grateful to The Ohio State University Instruction and Research Computer Center for providing computer time. M.H.K. is the recipient of a Research Career Development Award from the National Institutes of Health. Gifts from Dr. Henry Sonneborn III and Mrs. Marion Colwill toward the purchase of the GC-MS system are gratefully acknowledged.

References and Notes

(1) A. K. Balls and H. N. Wood, *J. Biol. Chem.*, **219**, 245 (1956); R. J. Foster *ibid.*, **236**, 2461 (1961); N. S. Issacs and C. Niemann, *Biochim. Biophys. Acta*, **44**, 196 (1960); R. M. Epand and I. B. Wilson, *J. Biol. Chem.*, **238**, 1718 (1963); P. W. Inward and W. P. Jencks, *ibid.*, **240**, 1986 (1965); M. L. Bender, G. E. Clement, C. R. Gunter, and F. J. Kezdy, *J. Am. Chem. Soc.*, **86**, 3697 (1964); F. Seydoux and J. Yon, *Eur. J. Biochem.*, **3**, 42 (1967); J. Fastrez and A. R. Fersht, *Biochemistry*, **12**, 2025 (1973); M. M. Werber and P. Greenzaid, *Biochim. Biophys. Acta*, **293**, 208 (1973).
(2) C. B. Sawyer, *J. Org. Chem.*, **37**, 4225 (1972).
(3) J. E. Baggott and M. H. Klapper, *Biochemistry*, **15**, 1473 (1976).
(4) H. L. Goering, J. T. Doi, and K. D. McMichael, *J. Am. Chem. Soc.*, **86**, 1951 (1964).
(5) C. B. Sawyer and J. F. Kirsch, *J. Am. Chem. Soc.*, **97**, 1963 (1975).
(6) S. Rosenberg and J. F. Kirsch, *Fed. Proc.*, **37**, 1296 (1978).
(7) B. S. Hartley and B. A. Kilby, *Biochem. J.*, **56**, 288 (1954); F. J. Kezdy and M. L. Bender, *Biochemistry*, **1**, 1097 (1962).
(8) Details to be published elsewhere.
(9) E. K. Thornton and E. R. Thornton in "Isotopes in Chemical Reactions", C. J. Collins and N. S. Bowman, Eds., Van Nostrand-Reinhold, New York (1970), p 213.
(10) M. L. Bender and J. V. Kilheffer, *Crit. Rev. Biochem.*, **1**, 149 (1973).
(11) N. O. Kaplan and M. Ciotti *Methods Enzymol.*, **3**, 253 (1955).

Chih-Lueh A. Wang, Charlotte M. Trout
K. C. Calvo, Michael H. Klapper*
Department of Chemistry, The Ohio State University
Columbus, Ohio 43210

Lan K. Wong
Department of Pharmacology, College of Medicine
The Ohio State University, Columbus, Ohio 43210

Received October 16, 1978

Tris(dialkylamino)sulfonium Enolates

Sir:

Anion reactivity in aprotic solvents enhances greatly by crown ether complexation of the metal counter cation or replacement of the metal ion by an onium ion. Recently intermediacy of naked enolate **2** had been claimed as the highly reactive species in the reaction of enol silyl ether **1** and quaternary ammonium fluorides.[1,2] Rigorously, however, it has remained unclear whether the reactive intermediate is truly the ammonium enolate **2** or the alternative, pentacoordinate silicon species **3**.[3] In addition inevitable contamination of water molecules in the quaternary ammonium salts does not permit unambiguous judgment regarding the reaction mechanism. We disclose here that use of a tris(dialylamino)sulfonium difluorotrimethylsiliconate as a source of fluoride ion acting as a powerful siliconophile can remove this difficulty, providing direct evidence for generation of enolate species from enol silyl ethers and fluoride ion.

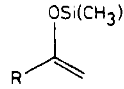

1

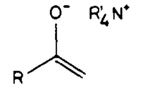

2

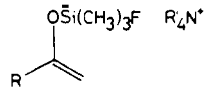

3

In order to examine this problem, we chose an enolate system which had been studied in detail by House.[4,5] The presence of a facile equilibrium outlined in Scheme I[6] allowed isolation of the enolate **8** utilizing a vacuum-line technique. An equimolar mixture of tris(diethylamino)sulfonium (TAS) difluorotrimethylsiliconate (**4**)[7] and the enol silyl ether **7** in THF solution was placed in a vessel connected with a vacuum line system. When this mixture was evacuated at 25 °C to 0.01 mmHg, 90% of the theoretical amount of fluorotrimethylsilane (**6**) was collected as THF solution in a cold trap (−78 °C). The residue obtained as extremely air-sensitive, yellowish crystals appeared

Scheme I

$$\underset{\mathbf{4}}{[(C_2H_5)_2N]_3S^+(CH_3)_3SiF_2^-} \rightleftharpoons \underset{\mathbf{5}}{[(C_2H_5)_2N]_3S^+F^-} + \underset{\mathbf{6}}{(CH_3)_3SiF}$$

$$\underset{\mathbf{5}}{[(C_2H_5)_2N]_3S^+F^-} + \underset{\mathbf{7}}{(Z)\text{-}C_6H_5CH{=}C(CH_3)OSi(CH_3)_3} \rightleftharpoons$$

$$\underset{\mathbf{6}}{(CH_3)_3SiF} + \underset{\mathbf{8}}{[(C_2H_5)_2N]_3S^+(Z)\text{-}C_6H_5CH{=}C(CH_3)O^-}$$

0002-7863/80/1502-1223$01.00/0

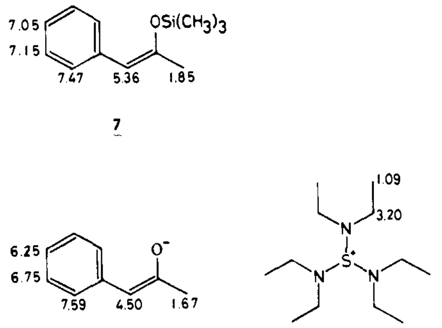

8

Figure 1. ^{1}H NMR data of the enol silyl ether **7** and the TAS enolate **8** (THF-d_8, parts per million downfield from tetramethylsilane internal standard).

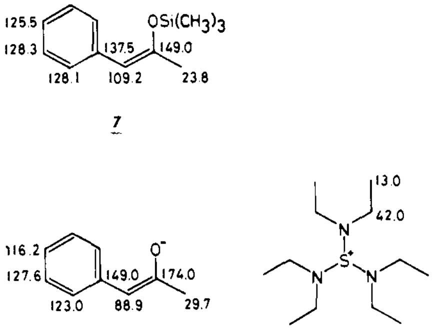

8

Figure 2. ^{13}C NMR data of the enol silyl ether **7** and the TAS enolate **8** (THF-d_8, parts per million downfield from tetramethylsilane internal standard).

to be the TAS (*Z*)-enolate **8**. The structure was firmly established by NMR analysis (Figures 1 and 2). Both ^{1}H and ^{13}C signals due to the TAS methylene group occurred at very low field,[8] eliminating the possibility of the covalent sulfurane structure. When a small amount of benzyl methyl ketone was present in the solution, rapid proton exchange between the ketone and the enolate took place and, as a result, considerable line broadening of the aromatic and vinylic ^{1}H signals was observed.[4,9] The TAS signals remained sharp, however.

Definitive evidence for ionic structure for **8** was obtained by conductivity measurements; the enolate **8** in THF showed a molar conductance of 1.80 cm^2 mol^{-1} Ω^{-1} at a concentration of 3.80×10^{-3} mol at 25 °C.

When NMR spectra of the enolate **8** are compared with those of the enol silyl ether **7**, one can see dramatic changes in chemical shift. As illustrated in Figure 1, ^{1}H signals arising from the vinylic proton and aromatic meta and para protons move upfield significantly. The ortho proton signal shifts downfield slightly. As is seen in Figure 2, the ^{13}C spectrum of **8** shows great upfield shifts for the vinylic, ortho, and para carbons, and substantial downfield shifts for the carbon attached to oxygen and aromatic ipso carbon. Since ^{1}H and ^{13}C(sp^2) chemical shift values for conjugated systems have profound correlation with electron density of the atoms,[10] the observed chemical shift changes should result mainly from delocalization of a negative charge.[11] The ab initio MO calculations with STO-3G minimal basis set were carried out on the model enol **9** and enolate **10**, and the electron distribution obtained is given in Figure 3.[12,13] The result indicates that, in going from **9** to **10**, all of the protons increase the electron density. Likewise π electron densities of the vinyl, ortho, meta, and para carbons enhance by the charge delocalization. On the other hand, introduction of a negative charge makes the ipso carbon and oxygen-bearing carbon the more *electron deficient.*

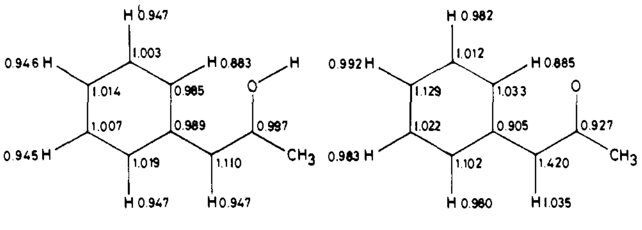

9 10

Figure 3. Calculated electron distribution in enol **9** and enolate **10** (1s for hydrogen and 2p$_z$ for carbon).

Thus the direction of the observed signal movement is mostly compatible with the change in electron distribution.[4,5,14,15] The magnitude of the chemical shift difference between the enolate and the neutral counterpart appears to be greater than any of the reported systems including crown ether complexed metal enolates.[16] This striking feature is attributed to the unique structure of TAS cation which possesses negligible interaction with the counteranion.[7,17]

Chemical behavior of the naked enolate is also to be noted.[18] When the TAS enolate **8** was treated with acetic anhydride in THF (1.2 equiv, −78 °C, 30 min), there was obtained only O-acylation product **11**[4] in 86% yield. By contrast, reaction of **8** and methyl iodide in THF (1 equiv, −78 °C min) led to the C-alkylation product **12** exclusively (85% yield). Notably the enolate **8** failed to react with benzaldehyde (1 equiv, −78 °C). After quenching of the mixture with water, no aldol adduct **13** was obtained, indicating that, unlike in the reaction of ordinary metal enolates, the equilibrium, **8** + $C_6H_5CHO \rightleftarrows$ **14**, lies so far to the left.[19] Fluorotrimethylsilane present in the reaction system, however, traps the anion **14** efficiently to form the aldol product **15**.[20]

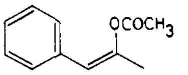

11

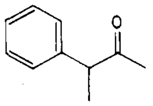

12

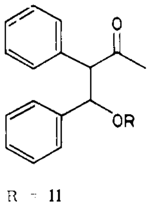

13, R = H
14, R = minus charge
15, R = Si(CH$_3$)$_3$

Acknowledgments. We are grateful to Dr. W. J. Middleton for his indication of the procedure for preparation of TAS difluorotrimethylsiliconate and Mr. M. Yamakawa for advice in the MO calculations. This work was supported in part by the Ministry of Education, Japanese Government (Grant-in-aid 403022).

References and Notes

(1) Kuwajima, I.; Nakamura, E. *J. Am. Chem. Soc.* **1975,** *97,* 3257.
(2) Noyori, R.; Yokoyama, K.; Sakata, J.; Kuwajima, I.; Nakamura, E.; Shimizu, M. *J. Am. Chem. Soc.* **1977,** *99,* 1265. Kleshick, W. A.,; Buse, C. T.; Heathcock, C. H. *Ibid.* **1977,** *99,* 247.
(3) Klanberg, F.; Muetterties, E. L. *Inorg. Chem.* **1968,** *7,* 155. Clark, H. C.; Dixon, K. R.; Nicolson, J. G. *Ibid.* **1969,** *8,* 450. Marat, R. K.; Janzen, A. F. *Can. J. Chem.* **1977,** *55,* 1167, 3845. Murphy, M. K.; Beauchamp, J. L. *J. Am. Chem. Soc.* **1977,** *99,* 4992.
(4) House, H. O.; Auerbach, R. A.; Gall, M.; Peet, N. P. *J. Org. Chem.* **1973,** *38,* 515.
(5) House, H. O.; Prabhu, A. V.; Phillips, W. V. *J. Org. Chem.* **1976,** *41,* 1209.
(6) The ^{1}H NMR spectrum of **6** (THF) shows the methyl signal at δ 0.20 as a doublet ($J_{CH_3,F}$ = 7 Hz), whereas **4** which is in a dynamic equilibrium with **5** and **6** affords a singlet at higher field, δ −0.14.
(7) Middleton, W. J. U.S. Patent 3 940 402, 1976.
(8) NMR of ionic TAS$^+$Br$^-$ showed ^{1}H signals at δ 1.28 (CH$_3$) and 3.51 (CH$_2$), and ^{13}C signals at δ 13.5 (CH$_3$) and 42.5 (CH$_2$), respectively.
(9) Pierre, J.-L.; Le Goaller, R.; Handel, H. *J. Am. Chem. Soc.* **1978,** *100,* 8021.
(10) Levy, G. C.; Nelson, G. L. "Carbon-13 Nuclear Magnetic Resonance for Organic Chemists"; Wiley-Interscience: New York, 1972; pp 22–24,

136–144. Stothers, J. B. "Carbon-13 NMR Spectroscopy"; Academic Press: New York, 1972; pp 208–238.

(11) Cf.: Bates, R. B.; Brenner, S.; Cole, C. M.; Davidson, E. W.; Forsythe, G. D.; McCombs, D. A.; Roth, A. S. *J. Am. Chem. Soc.* **1973,** *95,* 926. Ford, W. T.; Newcomb, M. *Ibid.* **1974,** *96,* 309. O'Brien, D. H.; Hart, A. J.; Russell, C. R. *Ibid.* **1975,** *97,* 4410.

(12) Planar structures are assumed for the models **9** and **10**, though in the actual compounds **7** and **8** two ortho and meta positions are equivalent in the NMR time scale. The structures for the calculations are derived using optimized (MINDO/3) bond lengths for vinyloxy anion (1.374 Å for C–C and 1.257 Å for C–O) and standard parameters for other fragments: Baird, N. C.; Dewar, M. J. S. *J. Chem. Phys.* **1969,** *50,* 1262. Bingham, R. C.; Dewar, M. J. S.; Lo, D. H. *J. Am. Chem. Soc.* **1975,** *97,* 1285.

(13) Since ^{1}H NMR spectra of phenol and phenyl trimethylsilyl ether exhibit same pattern in the aromatic region, use of the enol silyl ether as a neutral model compound would not be unreasonable.

(14) Fellmann, P.; Dubois, J.-E. *Tetrahedron Lett.* **1977,** 247. DePalma, V. M.; Arnett, E. M. *J. Am. Chem. Soc.* **1978,** *100,* 3514.

(15) Electron redistribution is certainly not the sole factor controlling the magnitude of the chemical shift change. The value in charged species is highly dependent on the nature of substituents, particularly heteroatoms: Olah, G. A.; White, A. M. *J. Am. Chem. Soc.* **1968,** *90,* 1884. Olah, G. A.; Halpern, Y.; Mo, Y. K.; Liang, G. *Ibid.* **1972,** *94,* 3554. The unusual behavior of the ortho proton signal would be a result of magnetic anisotropy of the oxygen atom.

(16) Reported chemical shifts (δ from internal tetramethylsilane) for the vinylic proton[4] and carbon[5] of the corresponding alkali metal enolates follow. ^{1}H: Li enolate, 4.83 (dimethyloxyethane); Na enolate, 4.86 (THF). ^{13}C: Na enolate, 97.1 (THF), 96.5 (THF + 12-crown-4); Na enolate, 90.7 (dimethoxyethane + dicyclohexano-18-crown-6); K enolate, 91.8 (dimethoxyethane).

(17) Farnham, W. B.; Middleton, W. J.; Sam, D. J. 172nd National Meeting of the American Chemical Society, San Francisco, Calif., Aug 30–Sept 3, 1976; American Chemical Society: Washington, D.C., 1976; ORGN 46. Cowley, A. H.; Pagel, D. J.; Walker, M. L. *J. Am. Chem. Soc.* **1978,** *100,* 7065.

(18) A recent review on the structure and reactivity of alkali metal enolate: Jackman, L. M.; Lange, B. C. *Tetrahedron,* **1977,** *33,* 2737.

(19) Ingold, K. U. "Structure and Mechanism in Organic Chemistry", 2nd ed.; Cornell University Press: Ithaca and London, 1969; Chapter 13.

(20) Evacuation of an equimolar mixture of **7** and tetrabutylammonium fluoride left the corresponding quaternary ammonium enolate. The ^{1}H NMR spectrum (THF-d_8) exhibited rather broad signals but was consistent with the assigned structure. The chemical shifts were intermediate between those of the Na enolate and TAS enolate. It should be added that the observation described herein does not generally exclude the possibility of formation of a pentacoordinate silicon species by reaction of an organosilicon compound and fluoride ion. Even in this case, we cannot decide rigorously whether the enolate generates from the enol silyl ether and fluoride ion via a concerted, S_N2-type mechanism or by way of a short-lived fluorosiliconate intermediate.

R. Noyori,* I. Nishida, J. Sakata, M. Nishizawa
Department of Chemistry, Nagoya University
Chikusa, Nagoya 464, Japan

Received October 4, 1979

Chemistry and Crystal Structures of Mixed-Valence Copper Dithioether Complexes with All-Tetrahedral Copper

Sir:

The idea of an entatic state in biological molecules is based on the premise that metal-ion-mediated electron-transfer processes will be most rapid when structural variations between oxidation states of the metal are small.[1,2] In plastocyanin[3] the copper has tetrahedral coordination, but this geometry is rare for Cu(II), especially in nonbiological molecules.[4] We report here the preparation, properties, and crystal structure of all-tetrahedral, mixed-valence copper complexes of 2,5-dithiahexane (2,5-DTH). The stoichiometry of the complexes is $Cu_2^{I}Cu^{II}(2,5\text{-DTH})_6(X)_4$ (X = ClO_4 and BF_4).[5] *The perchlorate salt is both shock and heat sensitive.* These deep green, mixed-valence complexes are unusual in that the preparation and crystal structures of both the red-brown, planar all-copper(II) complex of 2,5-DTH and the colorless, tetrahedral all-copper(I) complex have already been reported.[6] [Actually the structure of the 3,6-dithiaoctane (3,6-DTO) complex of copper(I) was reported owing to problems in obtaining a good crystal of the 2,5-DTH complex.]

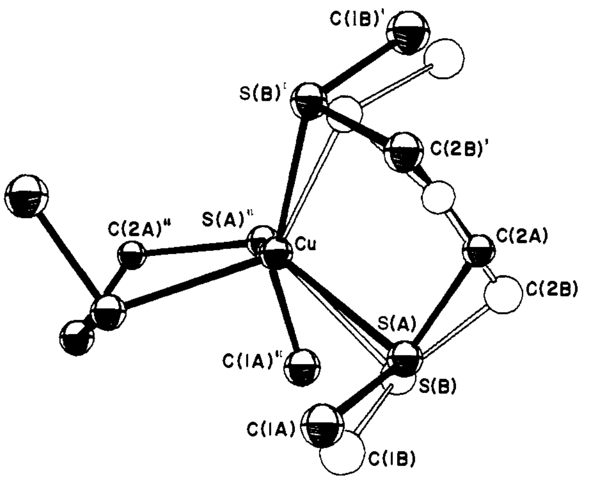

Figure 1. An ORTEP drawing of the $Cu(2,5\text{-DTH})_2$ cation showing 15% thermal ellipsoids. The disorder in one of the ligands is shown by the unshaded atoms. The $\bar{4}$ axis bisects a line between C(2B) and C(2B)′ and passes through Cu.

The red-brown, planar Cu(II) complex was originally prepared by Flint and Goodgame[7] by treating 2,5-DTH with $Cu(ClO_4)_2$ in *ethanol* in a ratio of 3:1. Under these conditions $Cu(2,5\text{-DTH})_2(ClO_4)_2$ precipitates immediately. Subsequent workers have followed this recipe.[8] By contrast, when the reaction is carried out in *methanol* at ~0.01 M $Cu(ClO_4)_2$ with a 2,5-DTH to copper ratio of ≤4:1, the initial solution turns deep green. Then slowly, deep green, lustrous crystals of the mixed-valence complex are deposited. An X-ray diffraction study of these crystals was carried out to confirm the stoichiometry, to determine the local geometry of copper, and to see whether a cluster was present.[9]

The results for the perchlorate salt (the tetrafluoroborate is similar) reveal a local tetrahedral geometry about each copper and no distinction between Cu(I) and Cu(II) complexes. That is, Cu(I) and Cu(II) must be randomly distributed in a disordered way, and the average oxidation state of copper is 1.33. This follows because the 12 copper atoms in the unit cell must occupy one set of special positions of point symmetry $\bar{4}$ (space group $I\bar{4}3d$, cubic). In this space group the $\bar{4}$ axis passing through copper bisects the C–C bonds, and the dihedral angle between S–Cu–S planes is required to be 90°. During the solution of the structure it became apparent that the ligand either undergoes large thermal motion or is disordered. Refinement carried out with anisotropic thermal parameters for S,C(1) and C(2) yields an *R* index similar to that obtained for a disordered model assuming a double set of atoms assigned weights of 0.5. In a formal sense our data do not permit a distinction to be made between static and dynamic disorder. However, since the distance between disorder positions for the C atoms is only ~0.5 Å, it is unlikely that a barrier exists which would cause a static disorder. We therefore assume the disorder to be dynamic. In any event, the two models yield identical averaged geometries, and we emphasize that this disorder in no way weakens the conclusion that there is a tetrahedral arrangement of sulfur atoms about copper. Packing forces have a well-known ability to influence the coordination geometry of Cu(II) complexes and apparently that is the case here, with Cu(II) trapped in a tetrahedral lattice site. The disordered configurations observed correspond to a twist of the C–C bond and a sideways displacement of the ligand, but little motion of the sulfur. This is illustrated for one of the two ligands in Figure 1. The internal S(A)–Cu–S(B) angle is 95 (1)°, and the external angles range from 111 to 123°. The observed angle between S–Cu–S planes is 90.2°. The average Cu–S distance is 2.28 (2) Å.

0002-7863/80/1502-1225$01.00/0